THE SEISMOLOGICAL SOCIETY OF AMERICA
400 Evelyn Ave., Suite 201
Albany, CA 94706-1375
(510) 525-5474; FAX (510) 525-7204
www.seismosoc.org

Bulletin of the Seismological Society of America, Vol. 105, No. 3, pp. 1810–1822, June 2015, doi: 10.1785/0120140294

Short Note

Sensitivity of Probabilistic Seismic Hazard Obtained by Algorithmic Differentiation: A Feasibility Study

by Christian Molkenthin, Frank Scherbaum, Andreas Griewank, Nicolas Kuehn, Peter J. Stafford, and Hernan Leovey

Abstract Probabilistic seismic-hazard analysis (PSHA) is the current tool of the trade used to estimate the future seismic demands at a site of interest. A modern PSHA represents a complex framework that combines different models with numerous inputs. It is important to understand and assess the impact of these inputs on the model output in a quantitative way. Sensitivity analysis is a valuable tool for quantifying changes of a model output as inputs are perturbed, identifying critical input parameters, and obtaining insight about the model behavior. Differential sensitivity analysis relies on calculating first-order partial derivatives of the model output with respect to its inputs; however, obtaining the derivatives of complex models can be challenging.

In this study, we show how differential sensitivity analysis of a complex framework such as PSHA can be carried out using algorithmic/automatic differentiation (AD). AD has already been successfully applied for sensitivity analyses in various domains such as oceanography and aerodynamics. First, we demonstrate the feasibility of the AD methodology by comparing AD-derived sensitivities with analytically derived sensitivities for a basic case of PSHA using a simple ground-motion prediction equation. Second, we derive sensitivities via AD for a more complex PSHA study using a stochastic simulation approach for the prediction of ground motions. The presented approach is general enough to accommodate more advanced PSHA studies of greater complexity.

Introduction

Probabilistic seismic-hazard analysis (PSHA) underpins a wide range of applications within the fields of earthquake engineering and engineering seismology. It is the basis for the seismic-hazard maps embedded within seismic code prescriptions, and its components are used extensively within probabilistic seismic risk analyses for both individual sites and spatially distributed portfolios. Having a clear understanding of which parameters drive the hazard results under various circumstances is therefore essential for understanding what parameters ultimately drive the results of these applications that build upon the hazard. In order to evaluate the impact that several inputs to PSHA have on the computed hazard, one needs to carry out a sensitivity analysis. Sensitivity analysis can identify critical inputs, provide insight to the model behavior, and help understand underlying mechanisms. This is important, particularly at the early stage of a PSHA where essential modeling decisions must be made. The Senior Seismic Hazard Advisory Committee (SSHAC; Budnitz *et al.*, 1997) report, which is a standard providing methodological guidance on how to conduct a PSHA in a proper way, emphasizes that sensitivity analysis for PSHA is crucial, both during the modeling process (for preliminary hazard calculations) and for understanding the final hazard results that are obtained.

Over recent decades, different approaches have been suggested to assess sensitivity issues in PSHA and for components of PSHA. The approaches that have been considered include using analytical expressions of the hazard integral for simple cases of PSHA (Cornell and Vanmarcke, 1969; Ordaz, 2004) and using factorial design (Rabinowitz and Steinberg, 1991); Cramer *et al.* (1996) carried out a sensitivity study for a regional seismic-hazard assessment by using classical Monte Carlo methods; Rabinowitz *et al.* (1998) pointed out the duality between an efficient construction of logic trees and sensitivity analysis in PSHA; Scherbaum *et al.* (2005) examined sensitivity issues based on Monte Carlo methods and a two-level factorial design regarding epistemic uncertainties in a key component of a PSHA, namely, ground-motion prediction; Rohmer *et al.* (2014) applied variance-based global sensitivity analysis relying on quasi-Monte

Carlo simulations to a regional earthquake loss assessment; and the SSHAC report gave examples of sensitivity analysis based on partial derivatives of the hazard results with respect to input parameters using finite-differences methods (Budnitz *et al.*, 1997).

However, techniques such as Monte Carlo methods, factorial design, or finite differences are often computationally demanding because their costs increase with the number of considered inputs. This can render these approaches infeasible for a large-scale PSHA. Therefore, herein, we demonstrate the use of an efficient method for differential sensitivity analysis (DSA), which is computationally feasible for large-scale seismic-hazard analysis because its computational cost is effectively independent of the number of inputs.

Typically, when performing a DSA, one calculates first-order derivatives of the model output with respect to its inputs; that is, one is interested in how small changes to the inputs affect the model output. Nevertheless, there exist complex models where the calculation of such derivatives is problematic, and thus sensitivity analysis becomes challenging. Differentiating by hand or even symbolically is often impossible or, at least, very tedious and error prone. Approximating the partial derivatives by finite differences is computationally expensive and is plagued by accuracy problems associated with the selection of the step size (cancellation error, truncation error). PSHA itself represents a complex model; therefore, we resort in this work to the use of algorithmic differentiation (AD; Griewank and Walther, 2008). This extremely powerful and flexible approach has been extensively used for performing sensitivity analyses of complex models in other domains such as oceanography (Marotzke and Giering, 1999) and aerodynamics (Gauger *et al.*, 2008). Two of the first applications using AD in seismology are from Sambridge *et al.* (2007) and Molkenthin *et al.* (2014). A major advantage of AD is that it can be applied directly on the computer source code representation of a model. In contrast to analytical differentiation, no clear set of explicit equations is needed. AD delivers highly accurate derivatives in an efficient manner through a source code transformation (Griewank *et al.*, 2012). Furthermore, introducing modifications or extensions to the code can be easily accommodated by AD with minimal programming effort. The AD methodology assumes continuous input variables and an input–output relation that is at least piecewise differentiable.

In this study, we employ AD to perform DSA for PSHA. To investigate the feasibility of using AD in the present context, we first study the sensitivities obtained analytically for the hazard integral of a point-source PSHA (Ordaz, 2004) with the sensitivities obtained via AD. Analytical solutions are only possible for highly idealized, or simplified, cases of PSHA where closed-form solutions of the hazard integral exist. In a second application, we evaluate sensitivities of PSHA in a more complex setting where derivatives cannot be obtained analytically. This latter example involves a PSHA for an area source, with a more sophisticated ground-motion attenuation model (as opposed to a simple ground-motion prediction equation [GMPE] employed in the first analytical case). Specifically, we use the ground-motion simulation technique based on the stochastic method (e.g., Boore, 2003). This method is widely applied in a broad range of applications in different tectonic regions in order to predict ground motions. In particular, ground-motion simulations based on the stochastic method are often employed in regions in which strong-motion data are scarce. The sensitivity analysis is undertaken by constructing the so-called adjoint model of the PSHA within the AD methodology. We derive relative sensitivity coefficients for different input parameters (seismicity parameters as well as those related to the ground-motion model). This study builds on the work of Ordaz (2004), which provided closed-form solutions for simple cases of PSHA, and the study of Molkenthin *et al.* (2014), which successfully implemented AD for a widely employed stochastic ground-motion simulation model in order to obtain sensitivities of response spectra using AD.

Algorithmic Differentiation and Differential Sensitivity Analysis

AD gauges how much a slight perturbation in the input parameters changes the model output. For simplicity, we assume a scalar model output y: for example, the annual rate of exceedance for a particular level of a response spectral ordinate at a fixed oscillator frequency:

$$y_0 = f(\boldsymbol{x}_0), \tag{1}$$

in which y_0 is the model output evaluated at $\boldsymbol{x}_0$, and $\boldsymbol{x}_0$ is a vector containing the values of the input parameters for the model. Mathematically, parameter sensitivities S_i are defined as the partial derivatives of the model output $f(\boldsymbol{x})$ (or y_0) with respect to each of its input parameters x_i:

$$S_i = \left.\frac{\partial f(\boldsymbol{x})}{\partial x_i}\right|_{\boldsymbol{x}0}. \tag{2}$$

The first-order nature of these expressions dictates that these sensitivities are inherently accurate only in very close vicinity of the reference point $\boldsymbol{x}_0$. Hence, DSA is geared toward assessing local sensitivities, which can be used for first-order uncertainty analysis.

Handling absolute sensitivities, like those computed above, in an importance analysis of the inputs can be misleading due to the fact that, in practice, fixed increments in the particular units of the basic variables x_i, correspond to very different levels of relative change for these variables. In order to remove the effects of different units or scales, one usually works with the so-called relative (logarithmic) sensitivities Φ_i. These are the absolute sensitivities S_i normalized by x_{0i}/y_0 (Frank, 1978; Saltelli, 2000):

$$\Phi_i = \frac{\partial \ln y}{\partial \ln x_i} = S_i \times \frac{x_{0i}}{y_0} \approx \frac{\Delta y}{y_0}\left(\frac{\Delta x_i}{x_{0i}}\right)^{-1}, \tag{3}$$

in which y_0 is the model output at the reference point $\boldsymbol{x}_0$, and x_{0i} is the ith component of $\boldsymbol{x}_0$. In this way, a percentage change of an input parameter is related to a percentage change of the model output.

The partial derivatives (equation 2) of the output of a complex model with respect to its inputs can be efficiently and accurately obtained via AD (Griewank *et al.*, 2012): for example, in the case of a general circulation model for an ocean (Marotzke and Giering, 1999). An additional, more contextually relevant, example of applying this approach is given by Molkenthin *et al.* (2014), in which sensitivities for predicted ground motions computed using the Stochastic Method SIMulation (SMSIM; Boore, 2003) technique are obtained. AD is a chain-rule-based method and has the advantage that it can, in principle, be applied directly to existing computer code of a model, irrespective of the model complexity. AD differentiates program code automatically using a compilerlike process (source code transformations). The transformed source code not only represents the model output itself but also the required derivative values (sensitivities) in floating point arithmetic. Subsequently, the transformed source code can be compiled by standard compilers into executable code.

The basic idea behind AD is that every computer program can be seen as the composition of a finite set of elementary calculations or instructions φ_i, computing a chain of intermediate values $v_i = \varphi_i(v_j)_{j \prec i}$, before the final output y is returned. Each value v_i is obtained by applying an operation φ_i to some set of arguments v_j, with v_j being a direct predecessor of v_i (denoted by $j \prec i$ as direct dependency of v_i on v_j) and, consequently, $\partial \varphi_i / \partial v_j \neq 0$.

This sequence of instructions in a computer code algorithm is realized programmatically by a set of intrinsic functions (e.g., sin, cos, exp) and arithmetic operations (e.g., $\times$, $+$, $-$):

$$\varphi_i \in \{\times, +, -, /, \sqrt{\cdot}, \sin, \cos, \exp, \ldots\}. \tag{4}$$

The repeated application of the chain rule to this sequence yields the desired partial derivatives of the model output with respect to its inputs. At the elementary level, the rules of differential calculus for arithmetic operations (e.g., the product rule) and a library of derivatives for the intrinsic functions (symbolic differentiation) are used.

The chain rule, due to its associativity, can be applied in two directions: (1) in the forward mode (that is, starting at input $\boldsymbol{x}$ and working toward output y), like in the original model); or (2) in the reverse mode of the original evaluation. The forward mode of AD gives the tangent linear model (TLM), whereas the reverse mode results in the adjoint model (ADM). The computational costs for calculation of the partial derivatives by TLM increase linearly with the number of inputs $O(n)$, in which n is the number of inputs. In contrast, using ADM in the case of a scalar-valued output, one can evaluate the complete gradient of the model output independently of the number of inputs with minimal overhead $O(c)$ (usually $c < 6$) (Griewank and Walther, 2008). All partial derivatives together with the model output can be evaluated in only one run of the ADM. ADM requires knowledge of the intermediate values v_i in reverse order. Thus, the reverse mode of AD consists of two stages: the forward sweep, which derives and stores the intermediates v_i; and the return sweep, when the chain rule is applied in reverse. Generally speaking, the program reversal in the return sweep as well as the required storage of the intermediates can be a major challenge for highly complex models.

Table 1

Example of Algorithmic Differentiation for $y = f(\boldsymbol{x}) = x_1 \cos(x_1 + x_2)$: Original Evaluation Code, Tangent Linear Model, and Adjoint Model

Original Code	TLM with Seeding for $\dot{y} = (\partial y / \partial x_1)$	ADM	Part of ADM
	Seeding: $\dot{x}_1 = 1$; $\dot{x}_2 = 0$		
$v_{-1} = x_1$	$v_{-1} = x_1$	$v_{-1} = x_1$	Forward sweep
	$\dot{v}_{-1} = \dot{x}_1$		
$v_0 = x_2$	$v_0 = x_2$	$v_0 = x_2$	
	$\dot{v}_0 = \dot{x}_2$		
$v_1 = v_0 + v_{-1}$	$v_1 = v_0 + v_{-1}$	$v_1 = v_0 + v_{-1}$	
	$\dot{v}_1 = \dot{v}_0 + \dot{v}_{-1}$		
$v_2 = \cos(v_1)$	$v_2 = \cos(v_1)$	$v_2 = \cos(v_1)$	
	$\dot{v}_2 = -\sin(v_1)\dot{v}_1$		
$v_3 = v_{-1} \times v_2$	$v_3 = v_{-1} \times v_2$	$v_3 = v_{-1} \times v_2$	
	$\dot{v}_3 = \dot{v}_{-1} \times v_2 + v_{-1} \times \dot{v}_2$		
$y = v_3$	$y = v_3$	$y = v_3$	
	$\dot{y} = \dot{v}_3$		
		$\bar{y} = 1$	Return sweep
		$\bar{v}_3 = \bar{y}$	
		$\bar{v}_2 = v_{-1} \times \bar{v}_3$	
		$\bar{v}_1 = -\sin(v_1) \times \bar{v}_2$	
		$\bar{v}_0 = 1 \times \bar{v}_1$	
		$\bar{v}_{-1} = 1 \times \bar{v}_1 + v_2$	
		$\bar{x}_1 = \bar{v}_{-1}$	
		$\bar{x}_2 = \bar{v}_0$	

TLM, tangent linear model; ADM, adjoint model.

In order to demonstrate the fundamental concepts of TLM and ADM, we present a simple illustrative example of AD for the function $y = f(\boldsymbol{x}) = x_1 \cos(x_1 + x_2)$ in Table 1. For a more comprehensive background to AD, we refer the interested reader to work by Griewank and Walther (2008). In Table 1, the first column shows the original code of the model. The model can be decomposed into six steps with five intermediate values v_i. The second column corresponds to the TLM of the source code, which is the original code augmented by statements to evaluate the derivatives $\dot{v}_i$ for each intermediate v_i. In the example, $\dot{x}_1$ is set to 1, whereas $\dot{x}_2$ is set to zero, which corresponds to a seeding in order to obtain the partial derivative $\dot{y} = (\partial y / \partial x_1) = 1 \times \cos(x_1 + x_2) + x_1 \times [-\sin(x_1 + x_2)] \times (0 + 1)$. Thus, one run of TLM gives one component of the gradient. Subsequently, the seeding is changed to compute the second component of the gradient ($\dot{x}_1 = 0$ and

$\dot{x}_2 = 1$) by a second run of TLM ($\dot{y} = (\partial y/\partial x_2) = 0 + x_1 \times [-\sin(x_1 + x_2)] \times (1 + 0)$). Hence, the evaluation of the complete gradient of a scalar-valued output requires n runs, in which n is the number of inputs needed in the model.

The last two columns of Table 1 present the ADM of the original code, with the forward sweep being a copy of the original code, and the return sweep with the program reversal and additional statements calculating the adjoints $\bar{v}_i = \partial y/\partial v_i$ for each intermediate v_i. A single run of the ADM calculates the adjoints $\bar{x}_1$ and $\bar{x}_2$, which correspond to the partial derivatives (complete gradient) of the model output with respect to its inputs ($(\partial y/\partial x_1) = \bar{x}_1 = 1 \times [-\sin(x_1 + x_2)x_1 \times 1 + \cos(x_1 + x_2)]$, $(\partial y/\partial x_2) = \bar{x}_2 = 1 \times [-\sin(x_1 + x_2)x_1 \times 1]$).

The analysis and the transformation of the computer code, as shown in Table 1, is done automatically by the AD tool. Nevertheless, one must keep in mind that current AD tools do not operate in a fully automated way where the user simply supplies code and the desired result follows. It is often the case that the code must be prepared in advance; for example, redefining function headers, returned values, and modules of code (like in our case).

For the differentiation of computer codes, several powerful and mature AD tools are freely available, mainly for FORTRAN or C codes. A link for a comprehensive overview of AD tools and AD methodology, as well as AD applications is given in Data and Resources. In our study, we applied the FORTRAN AD tool Tapenade (Hascoët and Pascual, 2004) because we used FORTRAN code to compute the PSHA. The source code for the hazard computation has been programmed stepwise, assuring at each stage that the differential dependencies in the code are clearly defined and are recognizable to the AD tool. In this way, the source code has been successively extended. The differentiated code at each stage was tested against analytical solutions or finite differences with decreasing step size to deliver correct derivatives. The time required to develop the computational model as described above is comparable to the time one would spend to develop the traditional source code in a conventional way. However, specific attributes of code elements (e.g., solvers for ordinary differential equations [ODEs] that have a strongly adaptive step-size selection) can sometimes produce erratic derivatives. This was the case we encountered when looking to apply AD to the source code of the ground-motion simulation model using the stochastic method (Boore, 2003). The problematic code elements first had to be identified, and then the related problems to apply AD on the source code could be addressed. For the particular example given above, the adaptive ODE solver was subsequently changed by another quadrature rule with fixed abscissas and weights in order to avoid problems with AD in the reverse mode. The source code transformation for the PSHA cases concerned in this study takes less than 12 s. The accuracy and correctness of ADM was corroborated via comparisons between derivatives it evaluates and those obtained by (1) analytical solutions, (2) finite numerical differences with decreasing step size, and (3) TLM. For the second application in this study (PSHA for an area source), the runtime of the TLM evaluating the partial derivatives of the scalar-valued model output with respect to 11 inputs is ≈20.9 times the runtime of the original (primal) model. On the other hand, the ADM requires only ≈5.6 times the runtime of the original model for the same task using a 2011 iMac with 8 GB of RAM and a 2.5 GHz processor.

Model for Seismic-Hazard Computation: PSHA

The seismic hazard at a site of interest is usually expressed in terms of the expected number of ground-motion exceedances per year at a specified target level a_T of an intensity measure. This number is called the annual rate of exceedance $\nu(a_T)$, and its inverse is the return period $T = 1/\nu(a_T)$. Typically, $\nu(a_T)$ is computed for different values for a selected ground-motion parameter a_T, and the resulting set of values collectively defines the hazard curve for the given intensity measure. This measure is most commonly a particular response spectral ordinate or the peak ground acceleration (PGA) (see Fig. 1a).

Annual rates of exceedance $\nu(a_T)$, which are of interest in hazard studies, generally range between 0.01 and 10^{-8} (although exceptions for serviceability and safety critical scenarios exist at either end of this range). Specifically, for critical facilities such as nuclear power plants or particular waste repositories, typical target rates are $\nu(a_T) \leq 10^{-6}$, whereas rates of $\nu(a_T) \approx 0.002$ ($T = 475$ years) or $\nu(a_T) \approx 0.0004$ ($T = 2475$ years) are typically considered for conventional buildings.

The current state of practice for deriving $\nu(a_T)$ is by means of PSHA (Cornell, 1968; McGuire, 2004). The results of a PSHA are dependent upon choices and modeling decisions related to the following components: (1) models for the geometrical characterization of possible earthquake sources, (2) models for the seismic activity of these sources, and (3) models to predict the distribution of ground motions for each considered earthquake scenario. The PSHA calculation is performed by integrating the probability of exceeding the target level of motion a_T over all earthquake scenarios.

In this formulation, the geometrical characterization of an earthquake source is given by a probability density function $f_R(R, \boldsymbol{\Theta}_{f_R})$ of possible source-to-site distances R, which is characterized by a given set of distribution parameters $\boldsymbol{\Theta}_{f_R}$. It is generally assumed that earthquake hypocenters are uniformly distributed within the source zone. The parameterization of f_R depends on the specific geometry of the source zone and will be given later for the geometrical settings considered in this study.

Second, the seismic activity (seismicity) in each potential source is usually given in terms of a magnitude exceedance rate $\lambda(M, \boldsymbol{\Theta}_\lambda)$, which refers to the average annual number of earthquakes with a magnitude equal to or greater than M generated in the source. The vector $\boldsymbol{\Theta}_\lambda$ includes all seismicity input parameters (described later) necessary to specify $\lambda(M, \boldsymbol{\Theta}_\lambda)$. The relative frequency of different earthquake magnitudes of the seismic source is modeled as a ran-

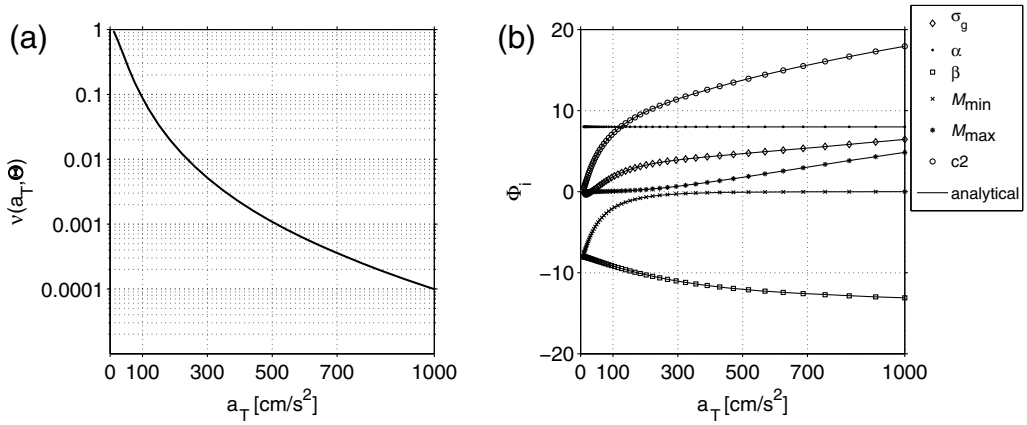

Figure 1. (a) Hazard curve $\nu(a_T, \boldsymbol{\Theta})$ for peak ground acceleration (PGA) considering a point source located at a distance of $R = 30$ km, $\sigma_g = 0.7$, and $\boldsymbol{\Theta}$ as given in Tables 2 and 3. (b) Comparison of analytically derived relative sensitivities of a probabilistic seismic-hazard analysis (PSHA) model (continuous line) with those evaluated via algorithmic differentiation (AD) methodology traced with markers. We note that the markers fall exactly on the continuous line.

dom variable with a source-specific probability density function $f_m(M, \boldsymbol{\Theta}_{f_m})$ in which the vector $\boldsymbol{\Theta}_{f_m}$ represents the input parameters that are required to define f_m.

In this study, we use a doubly truncated exponential distribution (the modified Gutenberg–Richter model) to characterize the seismic activity of a source, which can be parameterized based on $\boldsymbol{\Theta}_\lambda = [\alpha, \beta, M_{\min}, M_{\max}]$ as follows (McGuire, 2004):

$$\lambda(M, \boldsymbol{\Theta}_\lambda) = \lambda_{M_{\min}}(\alpha, \beta, M_{\min})[1 - F_m(M, \boldsymbol{\Theta}_{f_m})], \tag{5}$$

in which $\lambda_{M_{\min}}$ is the annual activity rate of the source (number of earthquakes per year with $M \geq M_{\min}$); F_m is the cumulative distribution function of the magnitude, and it is related to the integral of the probability density function $f_m(M, \boldsymbol{\Theta}_{f_m})$ with $\boldsymbol{\Theta}_{f_m} = [\beta, M_{\min}, M_{\max}]$; $\alpha = \ln(10) a_{\mathrm{GR}}$ is a measure of activity level (a value); $\beta = \ln(10) b_{\mathrm{GR}}$ represents the exponential decay rate of the distribution and controls the relative likelihoods of large and small magnitude earthquakes (b-value); and $M_{\min}$ and $M_{\max}$ represent the lower and upper limits of the truncation, respectively. The parameters a_{GR} and b_{GR} correspond to the parameters of the traditional Gutenberg–Richter relation that defines the number N of earthquakes of magnitude M or greater per unit time as $N(\geq M) = 10^{a_{\mathrm{GR}}} 10^{-b_{\mathrm{GR}} M}$. Correspondingly, the number of earthquakes per unit time with $M \geq 0$ is $10^{a_{\mathrm{GR}}} = \exp(\alpha)$.

The magnitude density f_m in our case corresponds to a doubly truncated exponential function (at $M_{\min}$, $M_{\max}$):

$$f_m(M, \boldsymbol{\Theta}_{f_m}) = \frac{1}{K} \beta \exp[-\beta(M - M_{\min})], \tag{6}$$

in which $K = 1 - \exp[-\beta(M_{\max} - M_{\min})]$. The activity rate $\lambda_{M_{\min}}$ is defined as

$$\lambda_{M_{\min}}(\alpha, \beta, M_{\min}) = \exp(\alpha - \beta M_{\min}). \tag{7}$$

The third part of a PSHA is the model that predicts the ground-motion distribution for each earthquake scenario. The level of shaking at a site due to an earthquake of magnitude M and source-to-site distance R is taken as a log-normally distributed random variable characterized by its two parameters μ_g (location parameter, mean of the logarithmic ground motion) and σ_g (scale parameter, standard deviation of the logarithmic ground motion). The two parameters are given by ground-motion models, usually empirically derived GMPEs.

Within the ground-motion model, the parameter $\mu_g = \mu_g(M, R, \boldsymbol{\Theta}_g)$ is given as a function of magnitude M, source-to-site distance R, and parameters included in $\boldsymbol{\Theta}_g$, in which the following relation between the mean of the logarithmic ground motion ($\mu_g(M, R, \boldsymbol{\Theta}_g)$) and the median of the ground motion, denoted by $g(M, R, \boldsymbol{\Theta}_g)$, holds $\mu_g(M, R, \boldsymbol{\Theta}_g) = \ln g(M, R, \boldsymbol{\Theta}_g)$. The second parameter σ_g (standard deviation of the logarithmic ground motion) that defines the lognormal distribution is often assumed to be constant across earthquake scenarios and is provided by the ground-motion model in terms of natural or base-10 logarithms, depending upon the formulation of the model. In this study, we use two different ground-motion models, or at least two different approaches to defining the ground-motion distribution, a simple GMPE that was used by Ordaz (1989), and a simulation-based ground-motion model representing an implementation of the stochastic method (Boore, 2003).

Finally, we compute the seismic hazard, following the Cornell–McGuire approach, for a single area source as follows:

$$\nu(a_T, \boldsymbol{\Theta}) = \lambda_{M_{\min}}(\alpha, \beta, M_{\min}) \int_R \int_{M_{\min}}^{M_{\max}} f_m(M, \boldsymbol{\Theta}_{f_m}) f_R(R, \boldsymbol{\Theta}_{fr}) \times Pr(A > a_T | M, R, \boldsymbol{\Theta}_g, \sigma_g) \mathrm{d}M \mathrm{d}R, \tag{8}$$

Table 2
Input Parameter Values of the Seismicity Model $\boldsymbol{\Theta}_\lambda = [\alpha, \beta, M_{\min}, M_{\max}]$

	Parameter			
	α	β	$M_{\min}$	$M_{\max}$
Value	8/yr	2	4	8

Table 3
Input Parameter Values of the Ground-Motion Attenuation $\boldsymbol{\Theta}_g = [c_1, c_2, c_3, c_4]$

	Parameter			
	c_1	c_2	c_3	c_4
Value	4.053	0.691	−1.000	−0.0071

in which $Pr(A > a_T|M, R, \boldsymbol{\Theta}_g, \sigma_g)$ is the probability that generated ground motion A at the site of interest exceeds the target level a_T for a given magnitude, distance, σ_g, and $\boldsymbol{\Theta}_g$. For simplicity, we are ignoring finite-fault effects.

By performing this integration, we take into account all possible hazard-relevant magnitude–distance scenarios. The probability, that a_T is exceeded, is given by

$$Pr(A>a_T|M,R,\boldsymbol{\Theta}_g,\sigma_g)=1-\Phi\left[\frac{1}{\sigma_g}\{\ln(a_T)-\ln[g(M,R,\boldsymbol{\Theta}_g)]\}\right] =\Phi\left[\frac{1}{\sigma_g}\ln\frac{g(M,R,\boldsymbol{\Theta}_g)}{a_T}\right], \quad (9)$$

in which $\Phi(\cdot)$ is the cumulative distribution function of the standard normal distribution $N(0, 1)$, and $g(M, R, \boldsymbol{\Theta}_g)$ is the median of the ground motion.

Sensitivity Analysis for the Point-Source Model of Ordaz (2004)

We first demonstrate the feasibility of deriving sensitivities for the hazard integral in PSHA via AD. For this purpose, we compare the obtained sensitivities using the AD methodology with those obtained analytically. Such a test is only possible for very simple cases of PSHA where closed-form solutions of the hazard calculation exist. To that end, we use the analytical expression for the hazard integral derived by Ordaz (2004) for a simple case of PSHA concerning a point source together with a simple ground-motion relation.

We derive the sensitivities (partial derivatives) of the model output $\nu(a_T, \boldsymbol{\Theta})$ with respect to its input parameters $\boldsymbol{\Theta} = [\alpha, \beta, M_{\min}, \ldots]$, according to equations (2) and (3), via both methods, whereas the analytical solutions are taken as the reference.

We use the same settings as Ordaz (2004). The point source is located at a source-to-site distance R. Given that we consider a point source and ignore rupture effects, there is only one distance that is relevant to our problem, and we can simplify our hazard integral to only consider an integration with respect to magnitude. Thus, equation (8) reduces to

$$\nu(a_T, \boldsymbol{\Theta}) = \lambda_{M_{\min}}(\alpha, \beta, M_{\min}) \int_{M_{\min}}^{M_{\max}} f_m(M, \boldsymbol{\Theta}_{f_m}) \times Pr(A > a_T|M, R, \boldsymbol{\Theta}_g, \sigma_g)\mathrm{d}M. \quad (10)$$

The seismicity of the source is characterized by a doubly truncated exponential Gutenberg–Richter model as given in equations (5), (6), and (7). The corresponding input parameter values are presented in Table 2.

We employ the same simple GMPE as Ordaz (2004), in order to describe the ground-motion attenuation of PGA (Ordaz, 1989):

$$\ln g(M, R, \boldsymbol{\Theta}_g) = c_1 + c_2 M + c_3 \ln R + c_4 R, \quad (11)$$

in which $g(M, R, \boldsymbol{\Theta}_g)$ is the median ground motion, R is the source-to-site distance, and $\boldsymbol{\Theta}_g = [c_1, c_2, c_3, c_4]$ are the coefficients of the GMPE, given in Table 3.

Solving the integral results in a closed-form solution for a point-source PSHA in terms of $\nu(a_T, \boldsymbol{\Theta})$ as follows (Ordaz, 2004):

$$\begin{aligned}\nu(a_T, \boldsymbol{\Theta}) = \frac{\lambda_{M_{\min}}(\alpha, \beta, M_{\min})}{1 - \exp(-\beta\Delta)} \Bigg[&\exp(\eta^2/2)\left[\frac{g(M, R, \boldsymbol{\Theta}_g)}{a_T}\right]^{\beta/c_2} \\ &\times \Bigg[\Phi\left(\frac{1}{\sigma_g}\ln\frac{g(M_{\max}, R, \boldsymbol{\Theta}_g)}{a_T} + \eta\right) \\ &- \Phi\left(\frac{1}{\sigma_g}\ln\frac{g(M_{\min}, R, \boldsymbol{\Theta}_g)}{a_T} + \eta\right)\Bigg] \\ &+ \Phi\left(\frac{1}{\sigma_g}\ln\frac{g(M_{\min}, R, \boldsymbol{\Theta}_g)}{a_T}\right) \\ &- \exp(-\beta\Delta)\Phi\left(\frac{1}{\sigma_g}\ln\frac{g(M_{\max}, R, \boldsymbol{\Theta}_g)}{a_T}\right)\Bigg], \end{aligned} \quad (12)$$

in which $\eta = \beta\sigma_g/c_2$ and $\Delta = M_{\max} - M_{\min}$.

For this simple case, partial derivatives (first-order absolute sensitivities) can be obtained analytically from equation (12). For example, the absolute sensitivity with respect to the parameter c_1 can be derived as follows:

$$\begin{aligned}\frac{\partial\nu(a_T,\boldsymbol{\Theta})}{\partial c_1} = \frac{\lambda_{M_{\min}}(\alpha,\beta,M_{\min})}{1-\exp(-\beta\Delta)} \times \frac{1}{\sigma_g}\Bigg[&\exp(\eta^2/2)\left[\frac{g(M,R,\boldsymbol{\Theta}_g)}{a_T}\right]^{\beta/c_2} \\ &\times[\delta_\varphi(M_{\min},M_{\max},R,\boldsymbol{\Theta}_g,\sigma_g,\eta,a_T) \\ &+\eta\delta_\Phi(M_{\min},M_{\max},R,\boldsymbol{\Theta}_g,\sigma_g,\eta,a_T)] \\ &+\varphi[\tilde{u}(M_{\min},R,\boldsymbol{\Theta}_g,\sigma_g,a_T)] \\ &-\exp(-\beta\Delta)\varphi[\tilde{u}(M_{\max},R,\boldsymbol{\Theta}_g,\sigma_g,a_T)]\Bigg], \end{aligned} \quad (13)$$

in which $\tilde{u}(M, R, \boldsymbol{\Theta}_g, \sigma_g, a_T) = \frac{1}{\sigma_g}\ln\frac{g(M,R,\boldsymbol{\Theta}_g)}{a_T}$, $\varphi(x)$ represents the probability density function of the standard normal distribution $\mathcal{N}(0, 1)$, and

Table 4
Sensitivities of the Annual Rate of Exceedance $\nu(a_T, \boldsymbol{\Theta})$ Derived Analytically and via the AD Methodology for a Target Level of $a_T = 490.5$ cm/s^2 for Peak Ground Acceleration (PGA)

Method	$\frac{\partial}{\partial a}\nu(a_T, \boldsymbol{\Theta})$	$\frac{\partial}{\partial b}\nu(a_T, \boldsymbol{\Theta})$	$\frac{\partial}{\partial M_{\min}}\nu(a_T, \boldsymbol{\Theta})$	$\frac{\partial}{\partial M_{\max}}\nu(a_T, \boldsymbol{\Theta})$	$\frac{\partial}{\partial c_1}\nu(a_T, \boldsymbol{\Theta})$	$\frac{\partial}{\partial c_2}\nu(a_T, \boldsymbol{\Theta})$	$\frac{\partial}{\partial c_3}\nu(a_T, \boldsymbol{\Theta})$	$\frac{\partial}{\partial c_4}\nu(a_T, \boldsymbol{\Theta})$	$\frac{\partial}{\partial \sigma_g}\nu(a_T, \boldsymbol{\Theta})$
Analytical	1.15631×10^{-3}	-6.93952×10^{-3}	-1.83291×10^{-5}	2.48881×10^{-4}	3.68041×10^{-3}	2.28607×10^{-2}	1.25178×10^{-2}	1.10412×10^{-1}	7.69995×10^{-3}
AD: ADM	1.15632×10^{-3}	-6.93961×10^{-3}	-1.83345×10^{-5}	2.48871×10^{-4}	3.68042×10^{-3}	2.28608×10^{-2}	1.25178×10^{-2}	1.10412×10^{-1}	7.69993×10^{-3}
AD: TLM	1.15632×10^{-3}	-6.93961×10^{-3}	-1.83345×10^{-5}	2.48871×10^{-4}	3.68042×10^{-3}	2.28608×10^{-2}	1.25178×10^{-2}	1.10412×10^{-1}	7.69993×10^{-3}

AD, algorithmic differentiation; ADM, adjoint model; TLM, tangent linear model.

$$\delta_{\varphi}(M_{\min}, M_{\max}, R, \boldsymbol{\Theta}_g, \sigma_g, \eta, a_T) = \varphi\left(\frac{1}{\sigma_g}\ln\frac{g(M_{\max}, R, \boldsymbol{\Theta}_g)}{a_T} + \eta\right) - \varphi\left(\frac{1}{\sigma_g}\ln\frac{g(M_{\min}, R, \boldsymbol{\Theta}_g)}{a_T} + \eta\right)$$

$$\delta_{\Phi}(M_{\min}, M_{\max}, R, \boldsymbol{\Theta}_g, \sigma_g, \eta, a_T) = \Phi\left(\frac{1}{\sigma_g}\ln\frac{g(M_{\max}, R, \boldsymbol{\Theta}_g)}{a_T} + \eta\right) - \Phi\left(\frac{1}{\sigma_g}\ln\frac{g(M_{\min}, R, \boldsymbol{\Theta}_g)}{a_T} + \eta\right).$$

In a similar manner, we obtain the sensitivities for all input parameters of the PSHA model analytically: that is, for all entries in $\boldsymbol{\Theta} = [\alpha, \beta, M_{\min}, M_{\max}, c_1, c_2, c_2, c_4, \sigma_g]$.

In addition, we constructed an ADM of the considered PSHA via AD in the reverse mode. Based on the ADM, we compute the sensitivities of $\nu(a_T, \boldsymbol{\Theta})$ with respect to the input parameters of the PSHA, according to equation (2).

The comparison of the sensitivities obtained via the two methods are depicted in Figure 1 and Table 4. We show the relative sensitivities of the input parameters for a point source, with a source-to-site distance of 30 km and the corresponding hazard curve. The base case values of the input parameters $\boldsymbol{\Theta}$ are given in Tables 2 and 3, and the standard deviation of the logarithmic ground motion is $\sigma_g = 0.7$ (in natural logarithmic units). The sensitivities obtained by AD are depicted by markers, whereas the analytically obtained sensitivities are shown as solid lines (Fig. 1). For the same setting, absolute sensitivities of $\nu(a_T, \boldsymbol{\Theta})$ with respect to $\boldsymbol{\Theta}$ are given in Table 4 for $a_T = 490.5$ cm/s$^2 \approx 0.5g$, in which g stands for the gravitational acceleration. Sensitivities are obtained (1) analytically, (2) using AD in the reverse mode (ADM), and (3) via AD in the forward mode (TLM). It can be easily seen that the results obtained from both methods are virtually identical.

Hazard Computation for an Area Source Using a Stochastic Ground-Motion Model: Sensitivity Analysis

In this section, we carry out a sensitivity analysis for the case of an area source with uniform seismicity and a geometry given in Figure 2, following the geometric settings of Ordaz (2004). The area source has the shape of a disk with a radius $R_{\max}$ and is situated at a depth of H beneath the site of interest (Fig. 2). Instead of using a simple GMPE like that used in the point-source example presented in the previous section, we use a more complex approach for modeling the ground motions, namely, the stochastic ground-motion simulation technique (e.g., Boore, 2003).

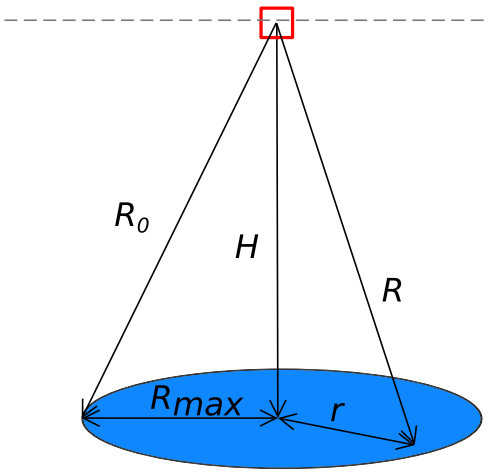

Figure 2. Geometric setting of the PSHA (in perspective view): area source (disk) with uniform seismicity and radius $R_{\max}$. The disk is situated parallel to the surface (dashed line) at depth H. The PSHA is computed at the site situated at the surface directly above the center of the area source. Each point source within the disk has a source-to-site distance $R = \sqrt{H^2 + r^2}$, in which r is the shortest distance between the point source and the center of the area source. The distribution of possible source-to-site distances is bounded by H (lower bound) and R_0 (upper bound). The color version of this figure is available only in the electronic edition.

A computer implementation of the stochastic method for ground-motion simulation is SMSIM (Boore, 2003). AD has been successfully implemented for SMSIM based on an enhanced version of its computer source code in order to obtain sensitivities of response spectra (Molkenthin *et al.*, 2014). For detailed information regarding AD of SMSIM the reader is referred to Molkenthin *et al.* (2014).

In this study, we employed the enhanced version of SMSIM that enables AD for this PSHA component. The following application demonstrates the flexibility and simplicity of the AD methodology for dealing with model adjustments or model extensions, for example, using more complex ground-motion models.

In order to calculate the hazard for an area source, one can assume uniformly distributed point sources over the source zone, each having a source-to-site distance $R = \sqrt{H^2 + r^2}$ and integrate their solutions for the whole area, in which r is the shortest distance between the assumed point source and the center of the area source (Fig. 2). After some manipulation (change of variables), the source-to-site distance distribution f_R can be derived analytically for the given geometry (Fig. 2) (Ordaz, 2004):

$$f_R(R, \boldsymbol{\Theta}_{f_R}) = 2R/R_{\max}^2. \tag{14}$$

For characterizing the seismicity of the source zone, we apply a doubly truncated exponential model according to equations (6) and (7). Thus, the hazard integral is

Table 5
Parametrization of WNA after Campbell (2003)

Parameter	WNA with $\boldsymbol{\Theta}_{\text{WNA}}$*
Source spectrum	Brune ω-square, point source
Stress parameter, $\Delta\sigma$ (bar)	100
Geometrical spreading, η	$1/R^{\eta} = 1/R$; $(\eta = 1)$
Ground-motion duration D_{gm} (s)	$1/f_c + 0.05R$
D_{rms} (s)	D_{gm}
Path attenuation quality factor $Q(f) = Q_0 f^{\alpha_q}$	$180f^{0.45}$; $(Q_0 = 180, \alpha_q = 0.45)$
Shear velocity, β_S (km/s)	3.5
Density, ρ_S (g/cc)	2.8
Site attenuating, κ_0 (s)	0.04
Site amplification	Generic rock site $V_{S30} = 620$ m/s Quarter-wavelength approximation

WNA, western North America
*Input parameters $\boldsymbol{\Theta}_{\text{WNA}}$ for western North America.

$$\nu(a_T, \boldsymbol{\Theta}, f_{\text{osc}}) = \exp(\alpha - \beta M_{\min}) \times \frac{2}{R_{\max}^2} \int_H^{R_0} \int_{M_{\min}}^{M_{\max}} \frac{\beta \exp[-\beta(M - M_{\min})]}{1 - \exp[-\beta(M_{\max} - M_{\min})]} R \times \Phi\left[\frac{1}{\sigma_g} \ln \frac{g(M, R, \boldsymbol{\Theta}_g, f_{\text{osc}})}{a_T}\right] \mathrm{d}M\,\mathrm{d}R, \tag{15}$$

in which H and R_0 are the limits for R, $g(M, R, \boldsymbol{\Theta}_g, f_{\text{osc}})$ is the median spectral acceleration, and f_{osc} stands for the natural frequency of a single-degree-of-freedom oscillator.

The ground-motion scaling is modeled using the stochastic method for ground-motion simulation (Boore, 2003). The target ground-motion parameter a_T is the spectral acceleration for a number of different oscillator frequencies. We employ a stochastic model that is based on Brune's source model (Brune, 1970, 1971), a stress parameter $\Delta\sigma$, and path and site attenuation filters (modeled by geometrical spreading $1/R^{\eta}$, a frequency-dependent quality factor $Q(f) = Q_0 f^{\alpha_q}$ and a site-specific κ_0), and the generic rock site amplification (Boore and Joyner, 1997; Cotton *et al.*, 2006) (see Table 5). Simple duration models are adopted. The parameter values are consistent with those typically used in western North America (an active tectonic setting) and are taken from Campbell (2003).

We note that our approach can also accommodate other attenuation relations (e.g., GMPEs) or other (more complex) stochastic models as well as other seismicity models or geometrical source characterizations besides the given choice here. Using GMPEs for describing ground-motion attenuation even simplifies the implementation of AD for PSHA, as GMPEs have a less complex structure than a stochastic ground-motion simulation model.

Below, we use AD to calculate sensitivities of $\nu(a_T, \boldsymbol{\Theta}, f_{\text{osc}})$ with respect to the seismicity parameters $\boldsymbol{\Theta}_{\lambda} = [\alpha, \beta, M_{\min}, M_{\max}]$, seismological parameters $\boldsymbol{\Theta}_g = [\Delta\sigma, \eta, Q_0, \alpha_q, \kappa_0]$, σ_g (standard deviation of the logarithmic ground motion), and H (depth of the area source),

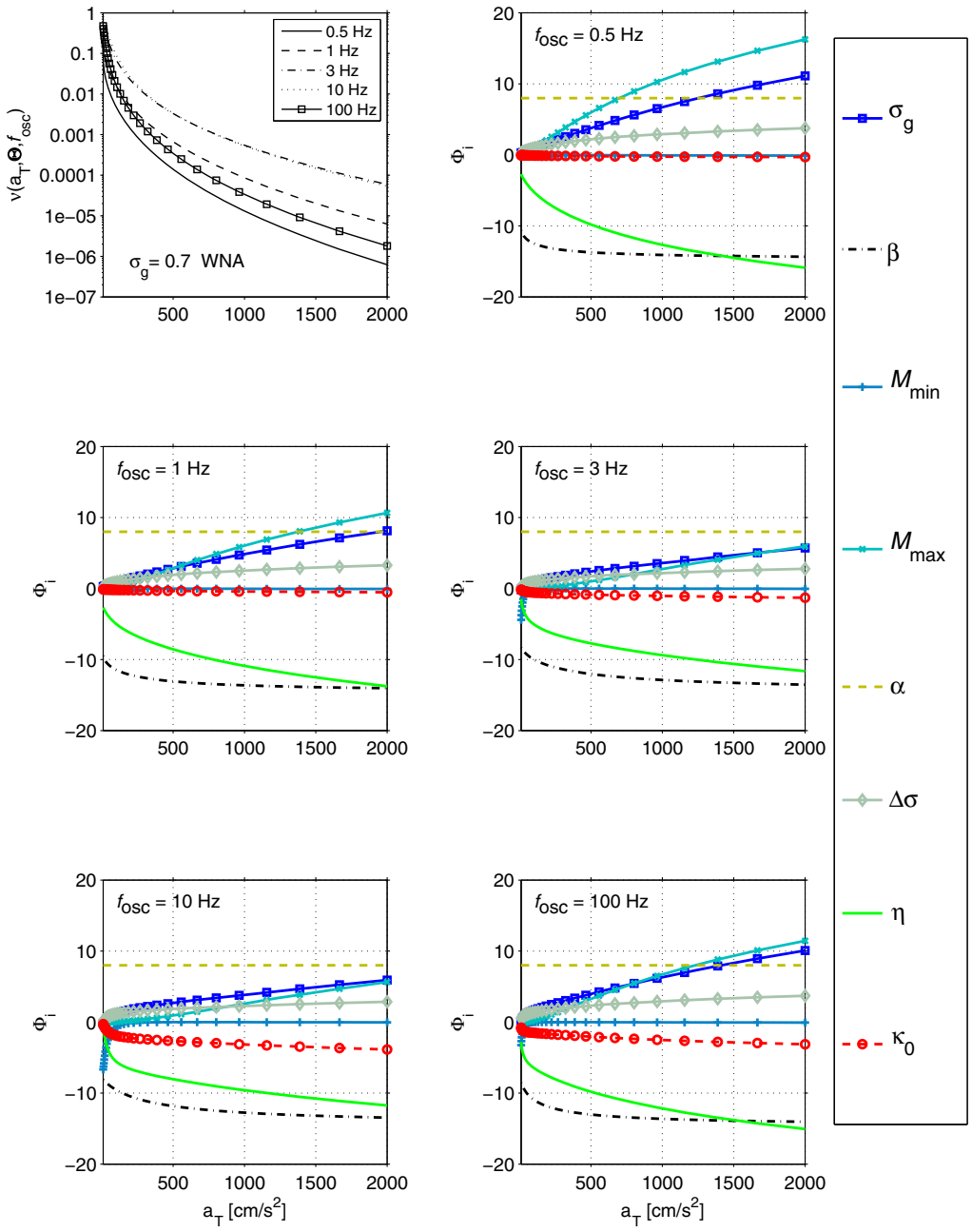

Figure 3. Relative sensitivities of $\nu(a_T, \mathbf{\Theta}, f_{\text{osc}})$ with respect to several input parameters of the PSHA model for different f_{osc} with following settings: $\sigma_g = 0.7$, $H = 20$ km, $R_{\max} = 30$ km. The corresponding hazard curves $\nu(a_T, \mathbf{\Theta}, f_{\text{osc}})$ are depicted in the first row, first column. Parameterization of the stochastic ground-motion model corresponds to western North America (WNA). The input parameters are α, β, minimum magnitude ($M_{\min}$), maximum magnitude ($M_{\max}$), standard deviation of the logarithmic ground motion (σ_g), exponent of the geometric spreading (η), stress parameter ($\Delta\sigma$), and site-specific high-frequency attenuation (κ_0). The color version of this figure is available only in the electronic edition.

according to equations (2) and (3). In the case of a general PSHA, partial derivatives (sensitivities) cannot be obtained analytically.

Figure 3 shows several hazard curves $\nu(a_T, \mathbf{\Theta}, f_{\text{osc}})$ and their corresponding relative (logarithmic) sensitivities with respect to a set of inputs for various f_{osc} using the previously described stochastic model for the ground-motion prediction. The input parameter values for the stochastic model are given in Table 5, and the standard deviation of the logarithmic ground motion is again taken as $\sigma_g = 0.7$. The seismicity parameters are given in Table 2. The geometric setting is defined by $H = 20$ km and $R_{\max} = 30$ km (Fig. 2), and the finite-rupture dimensions of events of all magnitudes are not considered.

From Figure 3, one can easily assess the impact of a slight relative change in each individual input on the hazard curve (relative change of the output) for different target

values a_T and for various natural frequencies f_{osc}. The direction of the influence (positive or negative sign) as well as a quantitative estimate in terms of a relative change of the output due to a slight relative change in the inputs (equation 3) are also given in Figure 3. For example, a slight relative increase in seismicity parameters $M_{\max}$ or α has a positive effect on the model output (increase of $\nu(a_T, \boldsymbol{\Theta}, f_{\mathrm{osc}})$), whereas a slight increase in β has a negative influence on $\nu(a_T, \boldsymbol{\Theta}, f_{\mathrm{osc}})$ for all a_T and f_{osc}.

As can be seen in Figure 3, the hazard curves for low a_T (equivalent to short return periods) are mainly influenced by seismicity parameters (β, α, $M_{\min}$) and the ground-motion attenuation parameter η (geometrical spreading). However, the influence of $M_{\min}$ on hazard curves is only present for low a_T in conjunction with high f_{osc} ($\geq$3 Hz), but it is still much lower than the impact of perturbing α or β. For low values of a_T, parameter $M_{\max}$ has a small impact on $\nu(a_T, \boldsymbol{\Theta}, f_{\mathrm{osc}})$. However, $M_{\max}$ becomes very important as a_T increases. The hazard curve $\nu(a_T, \boldsymbol{\Theta}, f_{\mathrm{osc}})$ is highly influenced by $M_{\max}$ for low f_{osc} (e.g., 0.5 Hz) at large values of a_T. With increasing f_{osc} the relative influence of $M_{\max}$ decreases and, in contrast to this, for very high f_{osc} (100 Hz) the relative sensitivity increases.

For large values of a_T, the influence of ground-motion attenuation parameters becomes stronger; the main influencing factors are η and σ_g. The sensitivities to these parameters vary with f_{osc}: sensitivities are large for both low f_{osc} (0.5 and 1 Hz) and high f_{osc} (100 Hz). The relative sensitivity to $\Delta\sigma$ is moderate, increasing with a_T and reveals hardly any dependency on f_{osc}. In contrast, the relative sensitivity to κ_0 shows a strong dependency upon f_{osc}. For low f_{osc} ($<$3 Hz), the influence of κ_0 is negligible, whereas for high f_{osc}, slight relative changes in κ_0 have a noticeable influence; the impact of κ_0 increases for large values of a_T.

The parameter σ_g has a significant influence on the computed hazard $\nu(a_T, \boldsymbol{\Theta}, f_{\mathrm{osc}})$ for large values of a_T. In addition, from Figure 4, we observe that σ_g affects the strength of the impact of $M_{\max}$. The relative sensitivities of $\nu(a_T, \boldsymbol{\Theta}, f_{\mathrm{osc}})$ to $M_{\max}$ decrease significantly as σ_g increases. This reflects the fact that as the aleatory variability σ_g of the ground motion prediction increases, the upper bound ($M_{\max}$) of the magnitude distribution becomes less influential.

A simple and straightforward approach to assess the change in the model output due to changes in the inputs would be directly through perturbation calculations. Perturbation calculation means perturbing an input (e.g., increasing or decreasing an input value) and subsequently calculating the change in the model output. Results are often depicted in so-called tornado plots, which show the influence of the different parameters using horizontal bars (Fig. 5). Such analyses can be very demanding from a computational perspective because the number of model runs increases linearly with the number of inputs. In Figure 5, we compare the change of the model output ($\nu(a_T, \boldsymbol{\Theta}, f_{\mathrm{osc}})$) obtained from a perturbation calculation for a change of $\pm$5% for each input

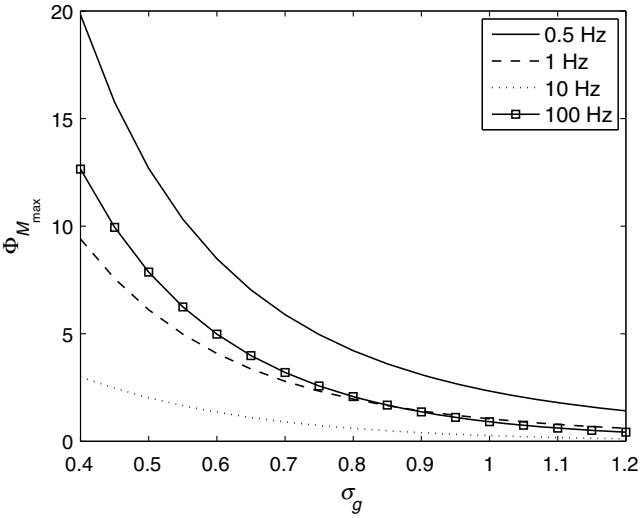

Figure 4. Relative sensitivities of $\nu(a_T, \boldsymbol{\Theta}, f_{\mathrm{osc}})$ with respect to $M_{\max}$ for different standard deviations of the logarithmic ground motion σ_g and several f_{osc} for $a_T = 490.5$ cm/s$^2 \approx 0.5g$ (g is gravitational acceleration). Parameterization of the stochastic ground-motion model corresponds to WNA. Seismicity parameters are given in Table 2.

with the sensitivities derived by using the ADM concerning first-order effects.

For the perturbation calculation, we compute the hazard ($\nu(a_T, \boldsymbol{\Theta}, f_{\mathrm{osc}})$) for a base case scenario using the parameter setting as described earlier (modified Gutenberg–Richter relation, area source, WNA stochastic model). Subsequently, we calculate the hazard by first changing one parameter at a time to its lower bound (-5%) and then to its upper bound ($+5\%$). It requires in total $2n + 1$ runs, in which n is the number of inputs. In contrast, the sensitivity-based estimate for the change in the model output, can be obtained by a single run of the constructed ADM of the PSHA independent of the number of inputs.

We considered 11 input parameters for the PSHA model ($\alpha, \beta, M_{\min}, M_{\max}, \sigma_g, \eta, \Delta\sigma, Q_0, \alpha_q, \kappa_0, H$). The results are shown as tornado plots for different values of a_T and f_{osc} (Fig. 5). In this particular case, the results depict how a change of 5% in the inputs effects the hazard estimates. The increased or decreased model outputs are given at the extremes of bars. The light-shaded bar corresponds to the calculated change of $\nu(a_T, \boldsymbol{\Theta}, f_{\mathrm{osc}})$ perturbing the corresponding parameter by $\pm$5%, whereas the dark-shaded bar gives the estimated change of the model output based on sensitivities. The vertical line gives the hazard for the base case.

The sensitivity-based estimates (dark-shaded bars) compare reasonably well with the computed changes (light-shaded bars) in the output from the perturbation calculations. One can observe that, for different values of a_T and f_{osc}, the ranking based on the scaled sensitivities coincide with the actual ranking computed for each perturbation. The quantitative estimates for the change in the model output based on the scaled sensitivities agree in an acceptable way for the

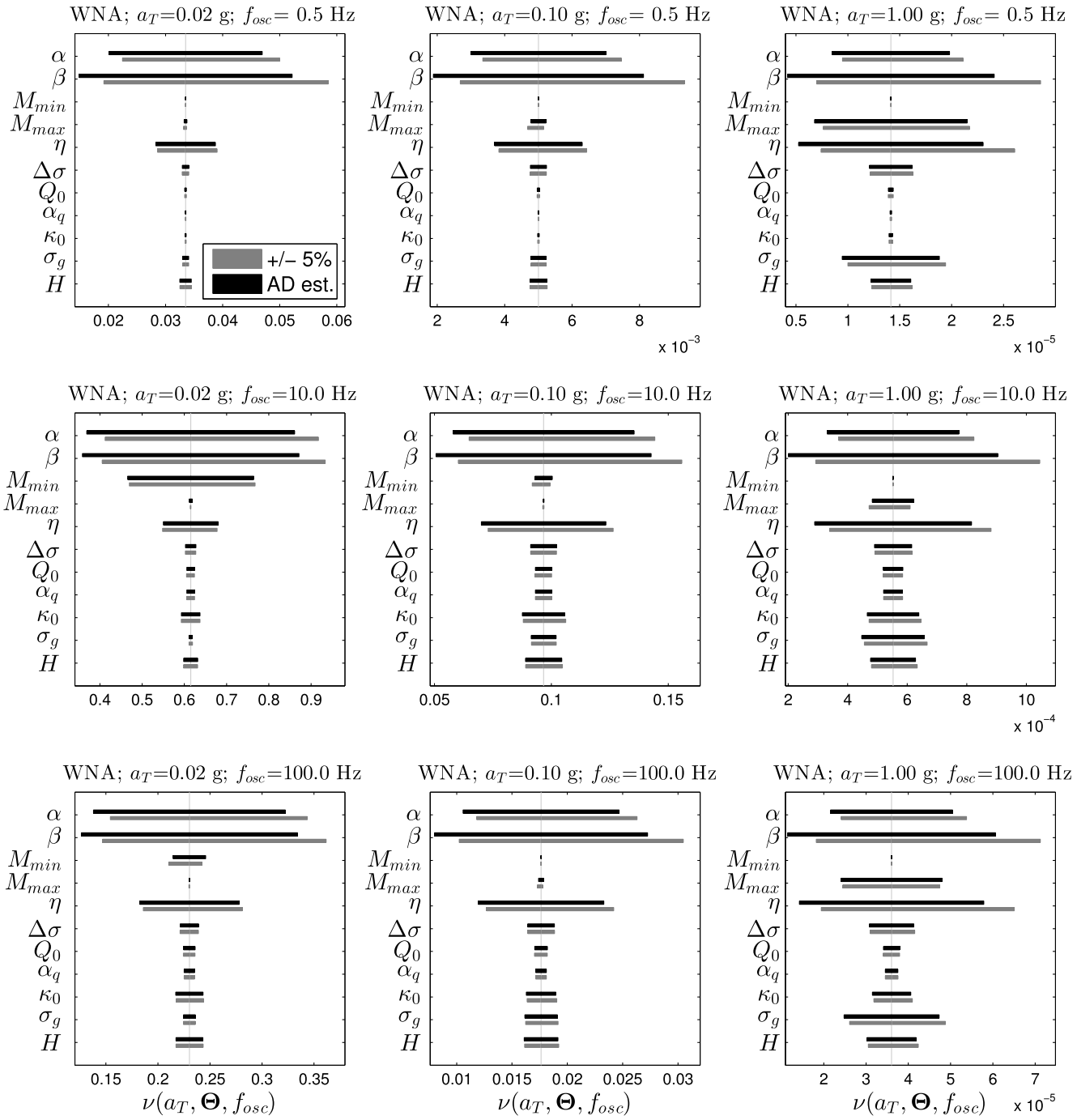

Figure 5. Tornado plots comparing the change of $\nu(a, \mathbf{\Theta}, f_{\text{osc}})$ due to 5% changes in the inputs (gray bars) with sensitivity estimates derived via AD (black bars) for different a_T and f_{osc} for the WNA case. The input parameters are α, β, minimum magnitude (M_{min}), maximum magnitude (M_{max}), standard deviation of the logarithmic ground motion (σ_g), exponent of the geometrical spreading (η), stress parameter ($\Delta\sigma$), parameters defining the frequency-depending quality factor (Q_0, α_q), site-specific high-frequency attenuation (κ_0), and depth of the area source (H).

input parameters. In the case of the parameters α, β, and η, the estimated change in the model output due to the perturbation in the inputs have to be treated with caution as the two approaches result in noticeable differences.

However, the ranking of the influencing factors and the overall picture regarding parameter importance are the same for the sensitivity-based estimates for the model change compared with the actual change of the model obtained by the perturbation calculation (concerning first-order effects).

Conclusion

Sensitivity analysis plays an important role for gaining insights into the behavior of a model and to assess the influence

of the model inputs on the model output. In this study, we showed how differential sensitivity analysis in PSHA can be carried out in an efficient way using AD. We illustrated the feasibility and applicability of AD for sensitivity analysis in the context of a closed-form solution PSHA using a simple GMPE. Subsequently, we also investigated the case of PSHA for an area source using a more complex ground-motion model based on a stochastic ground-motion simulation technique; for such a situation, the sensitivities cannot be derived analytically but are obtained efficiently via AD. The influence of the various input parameters on the hazard calculation is identified for different scenarios; primarily seismicity parameters (activity level α and exponential decay rate β) and geometric spreading influence the hazard result; for low annual rates of exceedance, small changes in other parameters predicting the ground-motion median and the ground-motion aleatory variability, as well as the depth of the source, have a significant impact. Nevertheless, one has to keep in mind that the DSA is a local method: it gives an estimate of first-order effects.

This study demonstrates the flexibility and efficiency of the AD approach for assessing sensitivities in PSHA. In particular, this becomes important in a real application of PSHA in which the number of input parameters increases rapidly with the number of sources, and the individual PSHA model components grow in complexity. The computational cost for the evaluation of the sensitivities via AD in the reverse mode is independent of the number of inputs. We feel that the results of this study illustrate the great potential of AD for use in PSHA. As a consequence, we are currently working on the application of the AD approach to a large-scale hazard code.

Data and Resources

The AD tool Tapenade http://www-sop.inria.fr/tropics/ (last accessed September 2014) is used for the algorithmic differentiation. Ground-motion simulations are based on a modified version of the FORTRAN source code Stochastic Method SIMulation (SMSIM) provided by David Boore http://www.daveboore.com/software_online.html (last accessed September 2014). A thorough overview of AD tools and AD methodology is given at http://www.autodiff.org (last accessed September 2014).

Acknowledgments

Christian Molkenthin is a fellow of the Helmholtz Graduate Research School, GeoSim, and wishes to thank the school for providing a scholarship. The authors are very grateful to Sebastian Reich, Nikos Gianniotis, Sanjay S. Bora, Annabel Händel, Matthias Ohrnberger, and Carsten Riggelsen for very helpful discussions and for their valuable suggestions, which led to improvements of the manuscript. The authors thank Marco Pagani and an anonymous referee, as well as Associate Editor Delphine D. Fitzenz, for many valuable comments and a thorough review that improved the manuscript. The first author is highly grateful to Isabella and August for their constant support and motivation.

This work was conducted in the Research Training Group GRK1364 "Shaping Earth's Surface in a variable Environment" funded by the German Research Foundation (DFG), cofinanced by the federal state of Brandenburg and the University of Potsdam.

References

Boore, D. M. (2003). Simulation of ground motion using the stochastic method, *Pure Appl. Geophys.* **160,** 635–676.

Boore, D. M., and W. B. Joyner (1997). Site amplifications for generic rock sites, *Bull. Seismol. Soc. Am.* **87,** 327–341.

Brune, J. N. (1970). Tectonic stress and the spectra of seismic shear waves from earthquakes, *J. Geophys. Res.* **75,** 4997–5009.

Brune, J. N. (1971). Correction to "Tectonic stress and the spectra, of seismic shear waves from earthquakes, *J. Geophys. Res.* **76,** 5002–5002.

Budnitz, R. J., G. Apostolakis, D. M. Boore, L. S. Cluff, K. J. Coppersmith, C. A. Cornell, and P. A. Morris (1997). Recommendations for probabilistic seismic hazard analysis: Guidance on uncertainty and use of experts, *U.S. Nuclear Regulatory Commission Report NUREG/CR-6372*.

Campbell, K. W. (2003). Prediction of strong ground motion using the hybrid empirical method and its use in the development of ground-motion (attenuation) relations in eastern North America, *Bull. Seismol. Soc. Am.* **93,** 1012–1033.

Cornell, C. A. (1968). Engineering seismic risk analysis, *Bull. Seismol. Soc. Am.* **58,** 1583–1606.

Cornell, C. A., and E. H. Vanmarcke (1969). The major influences on seismic risk, *Proc. of the Fourth World Conference on Earthquake Engineering*, Santiago, Chile, 13–18 January 1969, A-1, 69–93.

Cotton, F., F. Scherbaum, J. J. Bommer, and H. Bungum (2006). Criteria for selecting and adjusting ground-motion models for specific target regions: Application to central Europe and rock sites, *J. Seismol.* **10,** 137–156.

Cramer, C. H., M. D. Petersen, and M. S. Reichle (1996). A Monte Carlo approach in estimating uncertainty for a seismic hazard assessment of Los Angeles, Ventura, and Orange Counties, California, *Bull. Seismol. Soc. Am.* **86,** 1681–1691.

Frank, P. (1978). *Introduction to System Sensitivity Theory*, Academic Press, New York, New York, 386 pp.

Gauger, N. R., A. Walther, C. Moldenhauer, and M. Widhalm (2008). Automatic differentiation of an entire design chain for aerodynamic shape optimization, in *New Results in Numerical and Experimental Fluid Mechanics VI*, Springer, Berlin, Heidelberg, 454–461.

Griewank, A., and A. Walther (2008). *Evaluating Derivatives: Principles and Techniques of Algorithmic Differentiation*, Second Ed., SIAM, Philadelphia, 438 pp.

Griewank, A., K. Kulshreshtha, and A. Walther (2012). On the numerical stability of algorithmic differentiation, *Computing* **94,** 125–149.

Hascoët, L., and V. Pascual (2004). *TAPENADE 2.1 User's Guide, Technical Report, No. 0300*, Institut National de Recherche en Informatique et en Automatique (INRIA), Sophia Antipolis, 78 pp.

Marotzke, J., and R. Giering (1999). Construction of the adjoint MIT ocean general circulation model and application to Atlantic heat transport sensitivity, *J. Geophys. Res.* **104,** 29,529–29,547.

McGuire, R. K. (2004). *Seismic Hazard and Risk Analysis*, Earthquake Engineering Research Institute, Oakland, California.

Molkenthin, C., F. Scherbaum, A. Griewank, N. M. Kuehn, and P. Stafford (2014). A study of the sensitivity of response spectral amplitudes on seismological parameters using algorithmic differentiation, *Bull. Seismol. Soc. Am.* **104,** 2240–2252.

Ordaz, M. (2004). Some useful integrals in seismic hazard analysis, *Bull. Seismol. Soc. Am.* **93,** 1012–1033.

Ordaz, M., J. M. Jara, and S. K. Singh (1989). *Riesgo sísmico y espectros de diseño en el estado de Guerrero*, Report No 8782/9745, UNAM Instituto de Ingeniería (in Spanish).

Rabinowitz, N., and D. M. Steinberg (1991). Seismic hazard sensitivity analysis: A multi-parameter approach, *Bull. Seismol. Soc. Am.* **81,** 796–817.

Rabinowitz, N., D. M. Steinberg, and G. Leonard (1998). Logic trees, sensitivity analyses, and data reduction in probabilistic seismic hazard assessment, *Earthq. Spectra* **14,** 189–201.

Rohmer, J., J. Douglas, D. Bertil, D. Monfort, and O. Sedan (2014). Weighing the importance of model uncertainty against parameter

uncertainty in earthquake loss assessments, *Soil Dynam. Earthq. Eng.* **58,** 1–9.

Saltelli, A. (2000). What is sensitivity analysis? in *Sensitivity Analysis*, A. Saltelli, K. Chan, and E. M. Scott (Editors), Wiley, New York, New York, 1–12.

Sambridge, M., P. Rickwood, N. Rawlinson, and S. Sommacal (2007). Automatic differentiation in geophysical inverse problems, *Geophys. J. Int.* **170,** 1–8.

Scherbaum, F., J. J. Bommer, H. Bungum, F. Cotton, and N. A. Abrahamson (2005). Composite ground-motion models and logic trees: Methodology, sensitivities, and uncertainties, *Bull. Seismol. Soc. Am.* **95,** 1575–1593.

Institute of Earth and Environmental Science
University of Potsdam
Karl-Liebknecht-Str. 24-25
14476 Potsdam, Germany
molkenthin@geo.uni-potsdam.de
fs@geo.uni-potsdam.de
(C.M., F.S.)

Department of Mathematics
Humboldt-University Berlin
Unter den Linden 6
10099 Berlin, Germany
griewank@mathematik.hu-berlin.de
leovey@math.hu-berlin.de
(A.G., H.L.)

Pacific Earthquake Engineering Research Center
325 Davis Hall
University of California
Berkeley, California 94720-1792
kuehn@berkeley.edu
(N.K.)

Department of Civil and Environmental Engineering
Imperial College London
South Kensington Campus
London SW7 2AZ, UK
p.stafford@imperial.ac.uk
(P.J.S.)

Manuscript received 1 October 2014;
Published Online 26 May 2015